analytical chemistry

pubs.acs.org/ac

Article

A Portable 3D Microfluidic Origami Biosensor for Cortisol Detection in Human Sweat

Xuan Weng, Zhuoyi Fu, Cheng Zhang, Wen Jiang, and Hai Jiang*

Cite This: *Anal. Chem.* 2022, 94, 3526−3534

Read Online

ACCESS | Metrics & More | Article Recommendations

ABSTRACT: Analysis of cortisol levels in human sweat is increasingly important as it can be a "stress biomarker" in stress-related disorders, giving real-time information about human health status. In this study, a portable 3D microfluidic origami biosensor based on a smartphone was developed for cortisol-level detection in human sweat. Molybdenum disulfide (MoS_2) nanosheet-mediated fluorescence resonance energy transfer (FRET) and fluorescently labeled aptamers were employed in the biosensing process. A multilayer-structured 3D origami microfluidic chip was fabricated and functionalized to facilitate low-volume perspired human sweat collection, transportation, and detection. The translatability of the biosensor was exhibited by the fluorescence analysis in a smartphone mounted in a custom-designed holder. The critical design parameters of the microfluidic origami biosensor, including the characterization of various paper substrates, the concentration of MoS_2 nanosheets, and the incubation/reaction time, were adjusted to obtain an acceptable range for the assay dynamic range and limit of detection (LOD). Under optimum conditions, various doses of cortisol within the physiologically relevant range of 10−1000 ng/mL reported in human sweat were tested to evaluate the performance of the proposed biosensor. It displayed an LOD of 6.76 ng/mL at 3σ in artificial sweat, an analysis time of 25 min, and high selectivity. The performance of the proposed cortisol sensor was compared with an enzyme-linked immunosorbent assay (ELISA) for a spiked artificial sweat sample, and a correlation coefficient of 0.988 was found. The proposed biosensor also presented satisfactory results in the determination of the cortisol levels in a real human sweat sample. The resulting portable biosensor provides a rapid, low-cost, convenient, and non-invasive sensing solution for the point-of-care analysis of cortisol levels in sweat.

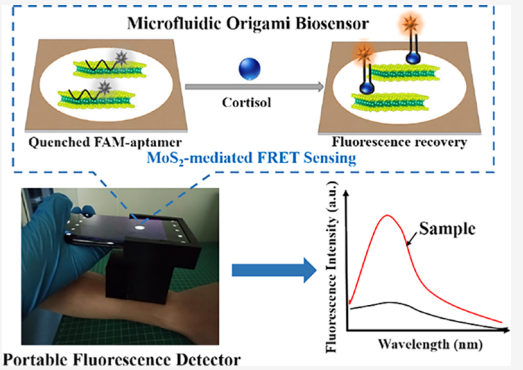

INTRODUCTION

With the ever-increasing development of society, the pace of life and work is speeding up and leads to increasing psychological stress.[1] Numerous studies show that stress has a broad impact on neuropsychiatric disorders and psychological and emotional strains, irrespective of age, gender, education, etc.; thus, the stress research is beneficial to the development of clinical interventions and health management.[2] Subjective stress is usually assessed as perceived stress and the stress-level quantification is traditionally measured by using self-rated questionnaires.[3] However, inaccurate perceptions of stress, inconsistencies in assessment, and low levels of objectivity have a strong impact on the outcomes of such questionnaires.[4] Measuring cortisol levels is an objective method of stress detection since it can be a biomarker that responds to both physical and psychological stress.[5,6] A normal range of cortisol level has been defined to be between 20 and 250 ng/mL, while the cortisol level in the body fluids follows a circadian cycle, which is at the peak during the daybreak and decreases by night-time.[7] Both high and low cortisol levels can disrupt the homeostasis of the immune system and be associated with diseases.[8] An active form of free cortisol can be found in the biofluids, including blood, sweat, urine, saliva, and interstitial fluid.[9] Traditional methods for cortisol detection in body fluids usually rely on centralized laboratory settings,[10−12] like gas/liquid chromatography and enzyme-linked immunosorbent assay (ELISA). Such methods are of high cost and are complex, multistep, and lengthy immunosensing procedures, although high sensitivity can be provided; thus, they are unsuitable for decentralized settings or point-of-care testing. Point-of-care diagnostic biosensors are capable of providing convenient ways for continuous personalized healthcare monitoring.[5,13,14] Compared to blood testing, sweat and saliva testing provides non-invasive stress hormone analysis without having a potential stress stimulus. Sweat is the preferred body fluid for point-of-care testing because it is easy

Received: October 18, 2021
Accepted: February 6, 2022
Published: February 16, 2022

https://doi.org/10.1021/acs.analchem.1c04508
Anal. Chem. 2022, 94, 3526−3534

to collect. In addition, the cortisol content in sweat changes periodically;[15,16] thus, immediate, accurate, and continuous measurement of cortisol levels in sweat can be used to evaluate the stress.

Electrochemical biosensors are characterized by their privileged merits of sensitivity, having label-free, miniaturization potential,[7] and have been reported to be used in the detection of cortisol.[17−19] Khan et al.[20] developed a highly sensitive electrochemical immunosensor for cortisol detection in saliva. The sensor consisted of gold (Au) microelectrodes coated with anticortisol antibody, poly(styrene)-*block*-poly(acrylic acid) (PS67-*b*-PAA27) polymer, and graphene nanoplatelet (GP) suspension coated on filter paper, and all were integrated in a printed circuit board (PCB). The sensor had a wide cortisol detection range from 3 pg/mL to 10 μg/mL and a sensitivity of 50 Ω $(\text{pg mL}^{-1})^{-1}$. Cheng et al.[17] developed a flexible electrochemical device for *in situ* detection of cortisol. The detection results of the volunteers' sweat samples could correctly reflect the cortisol rhythm of the human body via a confirmation by ELISA. Madhu et al.[18] presented an electrochemical immunosensor for cortisol detection, which was made of ZnO nanorod-coated flexible carbon yarns using a hydrothermal method. The immunosensor exhibited a linear detection range from 1 fg/mL to 1 μg/mL with the detection limit between 0.45 and 0.098 fg/mL. Although electrochemical sensors are able to provide high sensitivity, complex and costly fabrication and an immobilization procedure of microelectrodes are usually involved. More recently, many current cortisol determination strategies that rely on the microfluidic method with colorimetric detection have been developed. Apilux et al.[21] developed a low-cost paper-based immunosensor with competitive assay for detection of cortisol in serum. Gold nanoparticles (AuNPs) were used as a signal label for the colorimetric detection. The immunosensor was able to differentiate three ranges (<25 μg/dL, 25−50 μg/dL, and >50 μg/dL) of cortisol level by visual detection. Similarly, Dalirirad and Steckl[22] developed a lateral flow strip assay for cortisol detection in sweat. AuNPs modified with cortisol-selective aptamers were used as the color indicator for visual detection. The paper-based device covered a normal range of free cortisol in sweat (8−140 ng/mL). Pinto et al.[23] presented a microfluidic immunosensor combined with a metal-oxide-semiconductor (CMOS) system for colorimetric detection of salivary cortisol. The quantification was based on the competitive binding of horseradish peroxidase (HRP)-labeled cortisol and cortisol in the sample with the capture antibody. The microfluidic immunosensor demonstrated a linear range from 0.01 to 20 ng/mL, an LOD of 18 pg/mL, and an analysis time of 35 min. Using a microfluidic capillary flow assay, Vinitha et al.[24] detected unbound cortisol in saliva using a polymer lab-on-a-chip (LOC). The sensing was based on the microfluidic capillary flow assay, while the signal was detected by a portable fluorescence analyzer. The LOC was able to achieve a linear dynamic range of 7.0 pg/mL to 16.0 ng/mL. In addition to the electrochemical and colorimetric methods, Jo et al.[25] reported a surface plasmon resonance (LSPR) aptasensor for the detection of cortisol in saliva and a detection limit of 0.1 nM was obtained. However, the majority of above systems still suffer from complex fabrication, high-concentration (usually at millimolar level) analytes, and high costs or are solely characterized in artificial sweat samples.[26,27]

In this work, highly sensitive, selective, and efficient point-of-care cortisol sensing in human sweat was achieved through a 3D origami microfluidic device that combined the aptamer-based immunosensing, MoS_2 nanosheet-mediated FRET technique, and smartphone image processing system. The 3D origami microfluidic chip was made of hybrid paper substrates via the screen-printing technique followed by simple paper folding. Aptamers that are specific to cortisol and labeled with carboxyfluorescein (FAM) were employed as the biorecognition element, while MoS_2 nanosheets were employed as the fluorescence quencher. The morphological property of exfoliated MoS_2 nanosheets and the fluorescence quenching/recovering effects were investigated and characterized with scanning electron microscopy (SEM), atomic force microscopy (AFM), UV−Vis spectrometry, multifunctional enzyme plate analysis, and fluorescence microscopy. The background fluorescence intensity noise of various paper substrates, the influence of MoS_2 concentration on fluorescence quenching ability, and the reaction time were investigated to optimize the sensing performance of the proposed biosensor. Combined with a custom-designed smartphone-based fluorescence analysis system, the proposed biosensor could easily detect cortisol in both artificial and human sweat. Results demonstrated that the proposed 3D origami microfluidic biosensor was able to provide rapid, simple, and reliable detection of sweat cortisol for stress evaluation. Compared with most current detection methods, our method is suitable for use outside the laboratory. The wearable microfluidic patch and the portable detection device achieve all-weather detection in the daily life without any additional instrument and have strong adaptability to the environment. Although the LOC may not be superior to some costly analytical instruments (at pg/mL level for instance), our method is sufficiently competent to detect sweat cortisol as its detection range fully covers the cortisol level of the physiological state of the human body.

EXPERIMENTAL SECTION

Materials and Chemicals. Bulk MoS_2 was purchased from Shanghai Aladdin Biochemical Technology Co., Ltd. (100 g; #M104967; Shanghai, China). Cortisol was obtained from Solarbio Life Sciences Co., Ltd. (#C-93745, Beijing, China). Corticosterone was purchased from Shanghai Yuanye Biochemical Technology Co., Ltd. (#B65163, Shanghai, China). Artificial sweat was ordered from ChangFeng Technology Co., Ltd. (500 mL; #HE-3238, Dongguan, China). All other chemicals and reagents were of analytical grade and purchased from Shanghai Aladdin Biochemical Technology Co., Ltd. (Shanghai, China). The synthesized aptamer against cortisol (Sangon Biotech. Co., Ltd., Shanghai, China) was used as the sensing probe, the sequence of which was determined from a previous study,[28] as shown below:

FAM-5′-GGAATGGATCCACATCCATGGATGGG-CAATGCGGGGTGGAGAATGGTTGCCG-CACTTCGGCTTCACTGCAGACTTGACGAAGCTT-3′

The 5′-end was modified with the fluorescent dye 6-carboxyfluorescein (6-FAM). An ELISA kit for cortisol was purchased from Caobenyuan Biochemical Technology Co., Ltd. (#cby14234, Nanjing, China). Unless otherwise noted, all solutions were prepared by DI water. Regular printer paper was obtained from M&G Co., Ltd. (#APYVQ959, Shanghai, China). Coffee filter was purchased from SANYO Co., Ltd. (#V01, Fukuoka, Japan). Normal filter paper was purchased from Wohua Filter Paper Co., Ltd. (#M102, Hangzhou, China). Whatman #1 filter paper (W#1) was obtained from

https://doi.org/10.1021/acs.analchem.1c04508
Anal. Chem. 2022, 94, 3526−3534

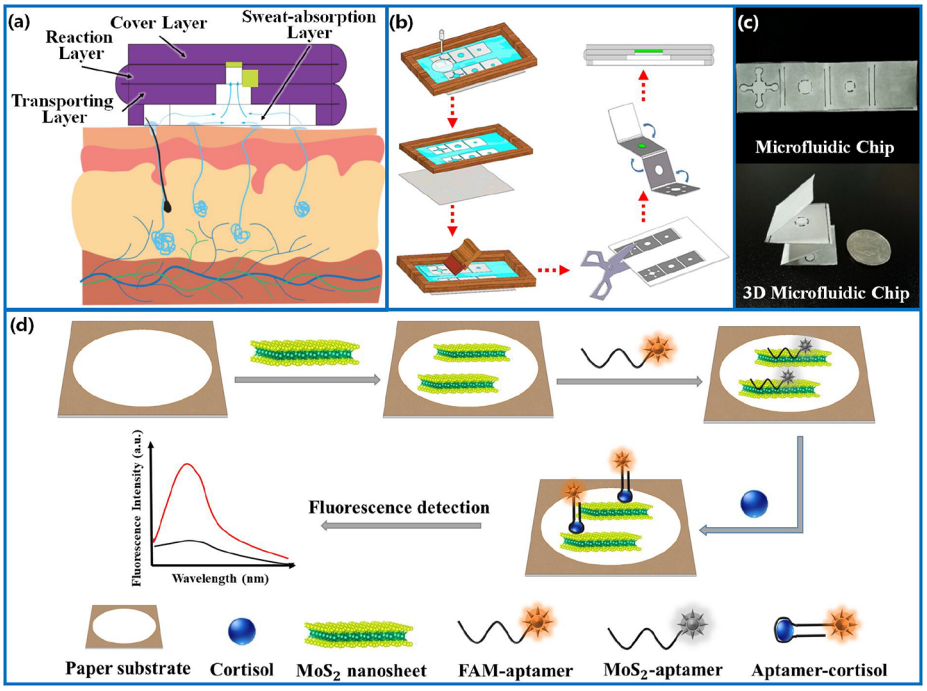

Figure 1. Schematic diagram of (a) sweat channels: sweat flows through horizontal and vertical channels and accumulates in the reaction layer. (b) 3D microfluidic origami chip made by screen printing, cutting, and folding. (c) Pictures of the four-layered microfluidic origami chip. (d) Schematic illustration of MoS_2-mediated FRET biosensing for cortisol levels.

GE Healthcare Life Science Co., Ltd. (#1823-025, Beijing, China). The nitrocellulose membrane was obtained from Zhongtian Electronics Co., Ltd. (#C_25, Dongguan, China).

Apparatus. Characterization of the bare MoS_2 nanosheets and the aptamer-decorated MoS_2 nanosheets was characterized by fluorescence microscopy (Olympus, IX73), scanning electron microscopy (SEM, VEGA3-SBH, TESCAN, Germany), atomic force microscopy (AFM, Bruker Dimension Icon, USA), and UV−Vis spectrophotometry (UV-2600i, SHIMADZU, Japan). The characterization of the fluorescence spectra was performed using a multifunctional enzyme plate analyzer (Thermo Scientific, Varioskan LUX). Pictures were acquired by a smartphone (Huawei, Mate30 Pro), followed by fluorescence intensity analysis using ImageJ. A custom-designed box for optical detection was fabricated by a 3D printer (Raise3D E2, Shang Hai, China) from a model drawn by SolidWorks. The excitation light source was provided by an LED lamp (LED ENGIN, LZ4-00B208). MoS_2 nanosheets were prepared by an ultrasonic cleaner (KQ3200DE, KUNSHAN Ultrasonic Instruments Co., Ltd., China) and a high-speed centrifuge (SIGMA, 3K15). Results of the ELISA test were read by a microplate reader (BioTek, ELX-808).

Preparation and Characterization of the Anticortisol Aptamer-MoS_2 Quenching System. The MoS_2 nanosheets were obtained by liquid exfoliation.[29] In a typical exfoliation process, 40 mg of MoS_2 powder was dispersed in 10 mL of DI water and stirred for 2 min at room temperature. The dispersion was then ultrasonicated for 10 h at 5 °C in the ultrasonic cleaner followed by centrifuging at 4500 rpm for 5 min to obtain MoS_2 nanaosheets. Finally, the supernatant was taken out and stored in the refrigerator at 5 °C for further use.

An aptamer stock solution (100 μM) was prepared by resuspending the original aptamer in TE buffer (10 mM Tris/1 mM EDTA). Prior to use, aptamers were folded into their active conformations. An aptamer working solution (100 nM) was made from the stock solution in the folding buffer (1 mM $MgCl_2$ and 1× PBS), followed by heating to 90 °C for 5 min and cooling to room temperature for use.

The anticortisol aptamer-MoS_2 quenching system was prepared by mixing the aptamer working solution with layered MoS_2 nanosheets followed by incubation at room temperature for a certain period. A series of layered MoS_2 nanosheets of various concentrations (i.e., 1, 2, 3, 4, 5, and 6 mg/mL) were tested to find out the optimal quencher concentration by evaluating the fluorescence quenching efficiency of MoS_2 nanosheets toward the dye-labeled aptamer.

Fabrication of the 3D Microfluidic Origami Device. The 3D microfluidic origami device consisted of four layers (as depicted in Figure 1a): (1) sweat-absorbing layer (filter paper, bottom layer) attached to the human skin, (2) transporting layer (filter paper, first intermediate layer), (3) reaction layer (nitrocellulose membrane, second intermediate layer), and (4) cover layer (filter paper, top layer), which was used to prevent the optical and chemical contamination. A microfluidic origami device was simply fabricated by the screen-printing technique and folding. The hydrophobic barriers on the filter paper substrate (Whatman No. 1, GE Healthcare) were made with polydimethylsiloxane (PDMS Sylgard 184, Dow Corning Corporation) by a screen-printing process (Figure 1b). Briefly, the microchannel patterns in the screen stencil were first designed and drawn using AutoCAD. A screen stencil bearing the microchannel patterns was then made from an 800-mesh polyester fabric on a wooden frame. To fabricate the hydrophobic barrier of microchannels, the paper substrate was placed under the screen stencil. The PDMS colloidal solution, which was prepared by mixing PDMS and crosslinker at a mass ratio of 10:1, was then rubbed onto the surface of the screen stencil and dragged across the whole length of the stencil with a squeegee. One sweep was sufficient for the penetration of PDMS colloidal solution across the paper

https://doi.org/10.1021/acs.analchem.1c04508
Anal. Chem. 2022, 94, 3526−3534

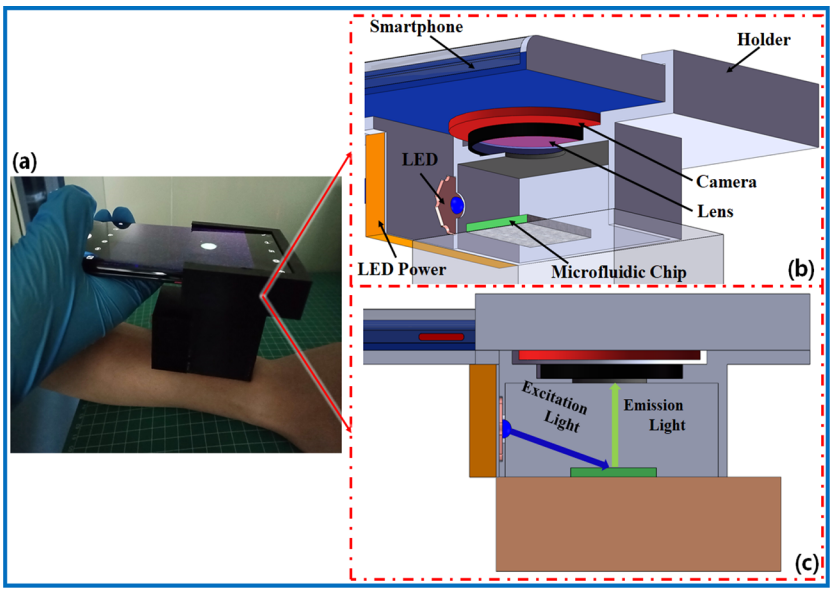

Figure 2. (a) Picture of the portable smartphone-based biosensor. (b) Schematic illustration of the components and structure of the proposed smartphone-based detection device. (c) Optical path diagram of the fluorescence analysis in the box.

substrate to form the hydrophobic barrier of microchannels. After printing, the paper substrate was dried out by curing at 60 °C for 2 h and then cooled down for further use. The residual PDMS in the screen was flushed with toluene to avoid blocking for repeated use. The patterned paper substrate was cut into the designed shape (10 cm × 2.5 cm, $l \times w$) and folded to create a 3D microfluidic chip. As shown in Figure 1c, the gray area was the hydrophobic layer with printed PDMS, and the white area was the clear filter paper. For the reaction layer, a circular reaction area was cut off and replaced by the nitrocellulose membrane of identical size (5 mm in diameter) due to its superior optical and diffusion properties compared to the filter paper.

Fluorometric Assay for Cortisol. The biosensing mechanism of the proposed biosensor was based on the fluorescence quenching and recovering properties of MoS_2 nanosheets through the FRET process relying on the adsorption and desorption of dye-labeled aptamers against cortisol,[30] as shown in Figure 1d. Briefly, layered MoS_2 nanosheets adsorb the 6-FAM-aptamer probes via the van der Waal force between the basal plane of MoS_2 and nucleobases,[31] resulting in the quenching of the fluorescence of the dye via energy transfer between them. In the presence of the target cortisol, a conformational change occurs when an aptamer hybridizes with its complementary target nucleotide to form double-stranded DNA due to the high affinity, leading to the aptamers being away from the surface of MoS_2 nanosheets, thus the recovery of fluorescence. Therefore, a quantitative readout of the target cortisol can be determined by analyzing the fluorescence intensity variation of the dye-labeled aptamers during the sensing process.

Before an assay, a 100 nM FAM-labeled aptamer was incubated with MoS_2 nanosheets at room temperature for 5 min to form the aptamer-MoS_2 probes. A droplet of aptamer-MoS_2 probes was added onto a well-cut nitrocellulose membrane and then embedded into the reaction layer of the microfluidic chip as the reaction area. In a typical assay, 10 μL of sample solution was added on the reaction area followed by an incubation. After the incubation, the cover layer was unfolded and the fluorescence intensity of the reaction zone was recorded by a smartphone-based analyzer (as shown in Figure 2).

Smartphone Readout and Image Data Processing. To acquire the fluorescence imaging and analysis, a custom-designed black box (7 cm × 6 cm × 8 cm, $l \times w \times h$) was fabricated by 3D printing for mounting the smartphone-based optical module, as shown in Figure 2a. The box clamped the top half of the smartphone, with its camera aligning to the sensing window where the image was captured. A schematic of the box for the microfluidic chip/optical component assembly and alignment can be seen in Figure 2b,c. An LED (488 nm) was mounted on the side of the box to provide the excitation light, while the camera mounted on the smartphone was used to record the emission light intensity from the reaction area through the bandpass filter (520 nm). A Li-ion battery was placed behind the LED as the power supply. The associated fluorescence intensity of the recorded images was then analyzed by ImageJ to obtain the concentration of the target object. In the study, the normalized fluorescence intensity (NFI) defined by $\Delta I = \frac{I_S - I_R}{I_R}$ was used in the fluorescence analysis, in which ΔI represents the normalized result, and I_R and I_S are the fluorescence intensity after quenching and recovery, respectively.

Optimization of the Proposed Biosensor. Major factors that significantly contributed to the performance of the proposed biosensor were studied. The properties of the paper substrate used for the fabrication of the microfluidic chip could affect the background fluorescence noise as well as the wicking of the sweat sample into the reaction site. The fluorescence noise of various paper substrates, namely, common printer paper (PP), coffee filter (CF), normal filter paper (FP), Whatman #1 filter paper (W#1), and nitrocellulose membrane (NC), was measured. With the paper substrate of the lowest fluorescence noise, the wicking capacity was tested to find out the minimum volume of the sweat sample required for the biosensor. In addition, the proposed biosensor was based on the MoS_2 nanosheet-mediated FRET

https://doi.org/10.1021/acs.analchem.1c04508
Anal. Chem. 2022, 94, 3526−3534

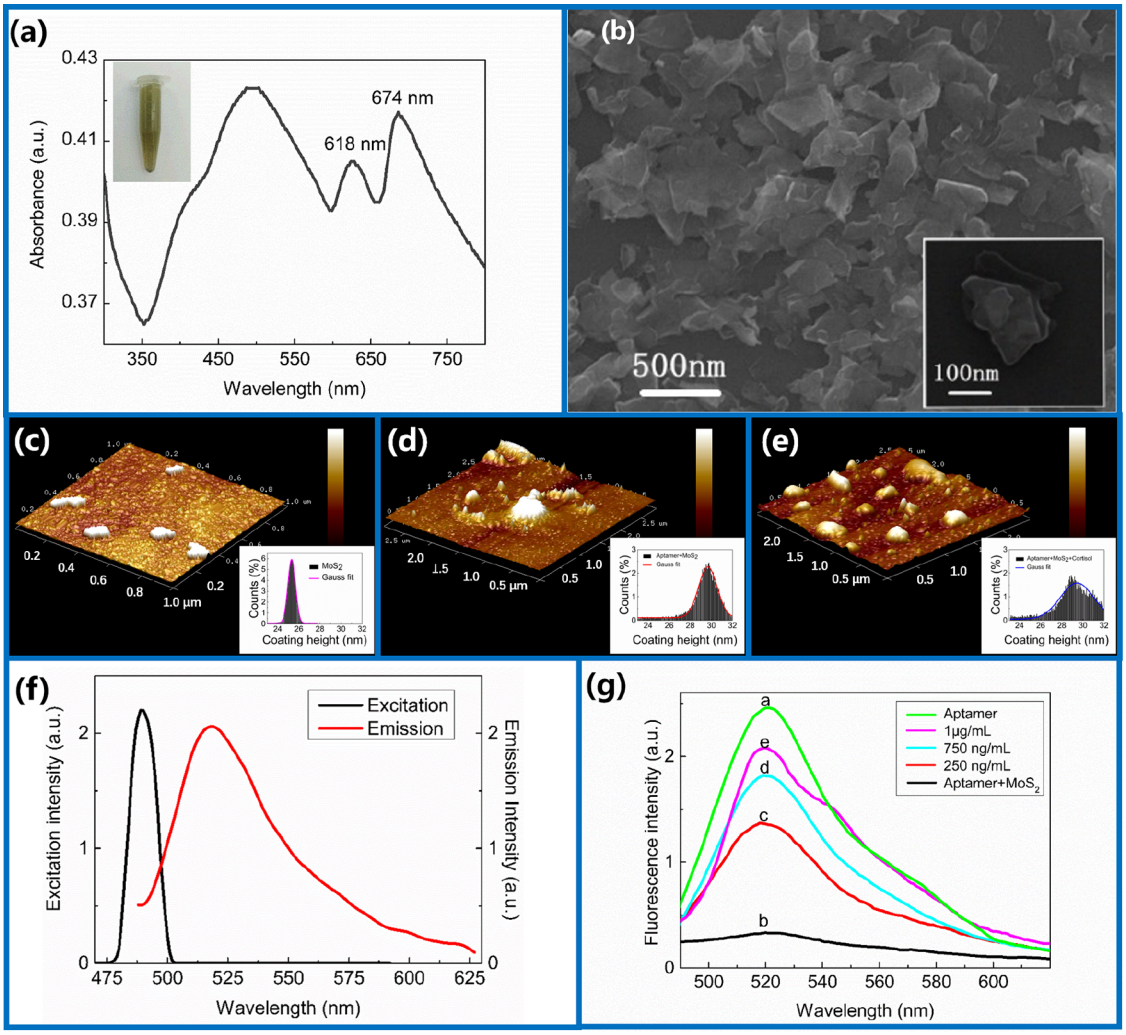

Figure 3. Characteristics of MoS_2 nanosheets and the 6-FAM-aptamer: (a) UV−Vis absorption peak of exfoliated MoS_2 nanosheets with an inset of MoS_2 nanosheet suspension. (b) SEM image of exfoliated MoS_2 nanosheets. AFM surface characterization of (c) MoS_2 nanosheets, of (d) aptamer-modified MoS_2 nanosheets, and (e) after exposure to cortisol. (f) Excitation and emission spectra of the 6-FAM-aptamer. (g) Fluorescence spectra of the 6-FAM-aptamer (curve a), aptamer-MoS_2 conjugates (curve b), and recovery fluorescence intensity for different cortisol concentrations (from curve c to curve e: 250, 750, and 1 μg/mL, respectively).

in the reaction process of fluorescently labeled aptamers and cortisol. Various concentrations of MoS_2 nanosheets (1 to 6 mg/mL), the incubation time (0 to 5 min), and reaction time (0 to 45 min) for fluorescence quenching and recovery were investigated to obtain the optimized sensitivity and efficiency.

Sweat Sample Collection and Preparation. Artificial sweat containing the key ingredients (minerals, amino acids, metabolites, etc.) and human sweat were tested in this study. Human sweat was collected from volunteers during physical exercise. The tests were approved by the Ethical Committee of University of Electronic Science and Technology of China (UESTC) and informed consent forms were signed by all subjects. Artificial sweat samples were spiked with standard cortisol solution ranging from 10 to 1000 ng/mL and then measured by both the proposed biosensor and gold-standard enzyme-linked immunosorbent assay (ELISA).

Interference Study and Validation. To demonstrate the specificity of the proposed biosensor, the common potential interfering substances present in sweat were investigated. Glucose (200 μM), lactic acid (20 mM), uric acid (10 mM), ascorbic acid (50 μM), Na^+ (100 mM), K^+ (50 mM), and corticosterone (1 μg/mL) solution were prepared in DI water and tested under the same conditions. A cortisol sample solution (100 ng/mL) in DI water was used as a reference for comparison.

To validate the performance of the proposed biosensor, the fluorescence analysis of cortisol samples was compared with that performed by a fluorescence microscope. In addition, the accuracy of our biosensor was further validated by a side-by-side detection of the cortisol levels in the spiked artificial sweat sample with a commercially available ELISA kit.

RESULTS AND DISCUSSION

Characterization of MoS_2 Nanosheets and Aptamer Probes. The few-layer MoS_2 nanosheets were obtained by liquid-phase exfoliation and centrifugation. The morphology of the layered MoS_2 nanosheets was characterized by UV−Vis spectrophotometry, SEM, and AFM. As seen in Figure 3a, a color change of suspension from dark gray to yellowish-green (shown in the inset) and two strong absorption bands at about 610 and 670 nm indicated the presence of the 2H polytype of MoS_2 nanosheets.[32,33] The SEM image (Figure 3b) reveals that

https://doi.org/10.1021/acs.analchem.1c04508
Anal. Chem. 2022, 94, 3526−3534

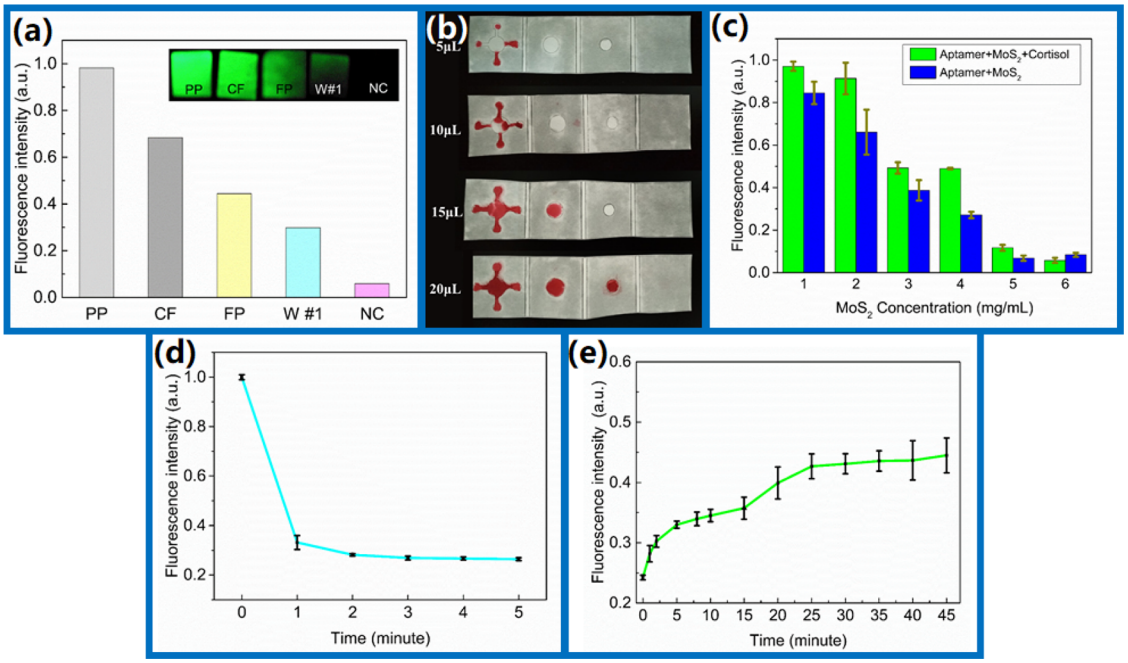

Figure 4. (a) Background fluorescence noise of various paper substrates. (b) Visualization of the fluid transportation process on the 3D microfluidic origami chip. (c) Influence of the MoS_2 concentration on the fluorescence quenching ability and fluorescence reproduction ability. (d) Fluorescence quenching process of the FAM-labeled aptamer by MoS_2 nanosheets. (e) Fluorescence reproduction process upon the detection of cortisol.

the MoS_2 nanosheets have a plain size ranging from 200 to 500 nm and the inset shows the sheet-like structure. To further characterize the MoS_2 nanosheets, aptamer-MoS_2 conjugates, and variation after exposure to cortisol, AFM analysis was performed (Figure 3c–e). The MoS_2 nanosheets were observed to have a sheet-like pattern and layered structure (Figure 3c). After addition of the aptamer (Figure 3d), the average height of MoS_2 nanosheets was found to increase from 25.8 to 29.3 nm, indicating the adsorption of the aptamers on the MoS_2 nanosheets via the van der Waal force. After exposure to cortisol (Figure 3e), aptamers hybridized with cortisol, causing their desorption from the surface of MoS_2 nanosheets due to the high affinity, resulting in the height decrease (28.1 nm) of MoS_2 nanosheets. The above results indicated the successful exfoliation and binging event in the whole reaction. The large surface area offered by the exfoliated MoS_2 nanosheets facilitated the biosorption and energy transition reaction in the sensing event. The FAM-aptamer was characterized by a multifunctional enzyme plate analyzer, as shown in Figure 3f; an excitation peak at ∼490 nm and an emission peak at ∼520 nm were observed. Therefore, a 520 nm narrow bandpass filter was mounted in the optical system to capture the emission light from the reaction area before being collected by the camera.

Mechanism Validation of the Aptamer-MoS_2 Conjugate-Based FRET Biosensor. The sensing mechanism of the proposed FRET-based biosensor was validated via the fluorescence spectrum analysis in a complete on-chip assay. The resulting fluorescence intensity of each step is presented in Figure 3g. Five microliters of FAM-labeled aptamer (100 nM) was first immobilized on the reaction area followed by the addition of 5 μL of MoS_2 nanosheets (4 mg/mL). After incubation, sample cortisol solutions of various concentrations were detected. The emission spectrum of the FAM-labeled aptamers showed an extremely strong peak at 520 nm (curve a). After the addition of MoS_2 nanosheets, the fluorescence intensity significantly decreased by 85% (curve b) due to the quenching effect of MoS_2 nanosheets. Upon the addition of cortisol, the recovery fluorescence intensity (curves c to e) was found to be associated with the cortisol levels; thus, it could be used to determine the concentration of cortisol in a sample.

Optimization. Since the proposed biosensor was based on a fluorescence detection, the optical noise must be reduced as much as possible. For example, the background fluorescence of the paper substrate due to the usage of fluorescent brighteners in the manufacturing process may significantly interfere with the actual fluorescence intensity, thus the accuracy and sensitivity of the biosensor. Five kinds of paper substrates, i.e., common PP, CF, normal FP, W#1, and NC, were tested to investigate their background fluorescence. As shown in Figure 4a, the nitrocellulose membrane presented the weakest background fluorescence noise. In addition to its fluorescence-friendly property, nitrocellulose membranes have high nucleic acid/protein-binding affinity.[34] Furthermore, the bilateral symmetrical cortex-free network structure enables the stable lateral chromatographic flow velocity on the nitrocellulose membrane, hence the rapid spread of the sample solution in this reaction area. Therefore, the nitrocellulose membrane was selected as the material for the reaction area. Since Whatman#1 filter paper has great hydrophilicity and good vertical dispersion but poor horizontal dispersion, it was used for the fabrication of the vertical microchannel layers. The "detached" reaction area allowed for independent decoration of probes and storage, providing convenience. In short, this design reduced the interference of the background fluorescence of the filter paper on the reaction results and enhanced the accumulation of the reagents in the filter membrane to avoid the diffusion in the microfluidic channel, thus improving the reaction accuracy.

https://doi.org/10.1021/acs.analchem.1c04508
Anal. Chem. 2022, 94, 3526−3534

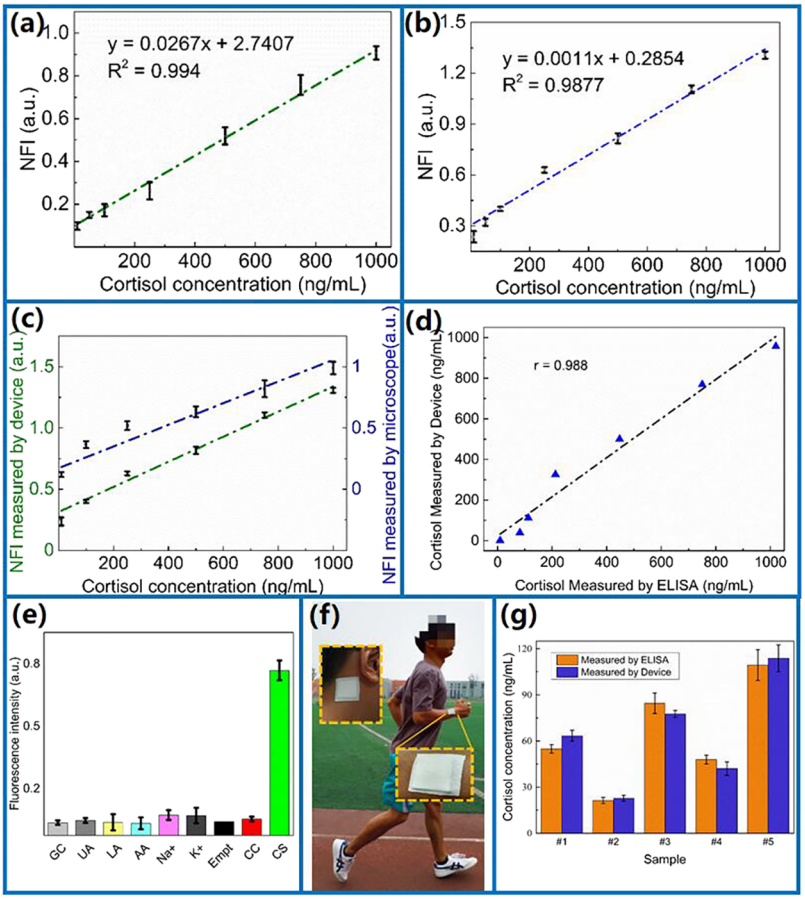

Figure 5. Calibration curve of cortisol in (a) DI water and (b) artificial sweat. (c) Validation of the optical measurement in cortisol detection with a smartphone-base detection device and fluorescence microscope. (d) Validation of the proposed smartphone-based biosensor toward cortisol-spiked artificial sweat detection with a commercial ELISA kit. (e) Specificity of the proposed cortisol (CS) biosensor against glucose (GC), uric acid (UA), lactic acid (LA), ascorbic acid (AA), Na^+, K^+, and corticosterone (CC). (f) A well-made 3D microfluidic origami chip was attached on the human skin for sweat collection. (g) Comparison of cortisol measurement of human sweat from five volunteers using a proposed biosensor and a commercial ELISA kit.

The absorbing and transporting properties of the 3D origami microfluidic device were investigated. Red ink was used to visualize the process of on-chip sweat transportation. Red ink of various volumes (5, 10, 15, and 20 μL) was loaded to the bottom sweat absorption area at an interval of 2 s to observe the filling process of the internal channels of a 3D well-made microfluidic chip. As shown in Figure 4b, the red ink pretty much flowed along the preset hydrophilic microfluidic channel, implying that the PDMS hydrophobic barriers effectively restrained the fluid. However, a minimum volume of 20 μL was required to fully fill the reaction area. Hence, 20 μL was considered as the minimum volume of the sample consumption. It was also observed that merely 2 s was required to have the liquid reach the reaction area. The test verified that our 3D microfluidic origami chip was able to effectively achieve the sweat absorption and transportation. Compared with other paper-based microfluidic channels,[35,36] our design is reasonable and compact, and it has the advantages of fast absorption rate and small sample consumption.

In the FRET-based sensing process, the concentration of MoS_2 nanosheets and the incubation/reaction time significantly affect the fluorescence quenching/recovery rate and efficiency, thus the detection sensitivity. Therefore, these parameters were optimized. Ten microliters of FAM-labeled aptamer (100 nM) was immobilized in the reaction area. MoS_2 nanosheets ranging from 1 to 6 mg/mL were studied by observing the fluorescence intensity change in the process of quenching and recovery in the detection of a cortisol sample (1 μg/mL). Incubation times for quenching and recovery were 5 and 30 min, respectively. The ratio between the quenching/recovery fluorescence and that before quenching were used to evaluate the performance. As shown in Figure 4c, fluorescence quenching occurred (10−90%) for all the studied concentrations. However, a greater difference between quenching and recovery fluorescence can provide better resolution, thus the high sensitivity. It was observed that the greatest intensity difference occurred at 4 mg/mL, while no significant difference was observed with higher concentrations. Therefore, the MoS_2 nanosheets (4 mg/mL) were used in the following tests. The time for fluorescence quenching and recovery may determine the total assay time and affect the sensitivity; thus, the incubation and reaction time were investigated to obtain an optimized performance. Results are presented in Figure 4d,e. In the tests, the FAM-labeled aptamer (100 nM) and MoS_2 nanosheets (4 mg/mL) were used in the detection of the cortisol sample (1 μg/mL). In the process of quenching, the fluorescence intensity was recorded at the time points of 0, 1, 2, 3, 4, and 5 min, respectively, with every 5 min in a period of 45 min in the process of recovery. It was found that a

https://doi.org/10.1021/acs.analchem.1c04508
Anal. Chem. 2022, 94, 3526−3534

significant change of quenching was exhibited at the time point of 2 min, with 20 min for the recovery process. Therefore, 25 min was considered the total assay time for a single test.

Optical Detection of Cortisol in the 3D Microfluidic Origami Biosensor. Under the optimized parameters, various cortisol solutions of standard concentrations (10−1000 ng/mL) in DI water (Figure 5a) and artificial sweat (Figure 5b) were tested to obtain the calibration curves. In both media, the recovery fluorescence intensity increased as the concentration increased. A good linear relationship was obtained between 10 and 1000 ng/mL cortisol, which could be expressed by the equations $y = 0.0267x + 2.7407$ and $y = 0.0011x + 0.2854$, respectively. The coefficients of determination (R^2) were 0.994 and 0.9877, respectively. The limits of detection of the proposed biosensor calculated by (3σ)/slope were 2.08 ng/mL (DI water) and 6.76 ng/mL (artificial sweat), which are within the normal range of cortisol in sweat.[37] The average standard deviation for all trials was less than 6% ($n = 3$), indicating acceptable repeatability.

The performance of the custom-designed smartphone detection device was validated by comparing their measurements with those by a fluorescence microscope (Olympus, IX73). As shown in Figure 5c, the measured output intensity of the mobile phone detection had a similar trend with that of the fluorescence microscope, however a little lower due to the hardware defects and errors. In addition, to validate the accuracy of our device, an artificial sweat sample spiked with standard cortisol solution ranging from 50 to 1000 ng/mL was measured with both the proposed biosensor and ELISA. The calculated LOD of the commercial ELISA kit was around 10.0 ng/mL. The levels of cortisol determined by ELISA and the proposed biosensor are listed in Table 1. The correlation analysis is performed and shown in Figure 5d; the horizontal axis presents the analysis result of ELISA, while the vertical axis presents those of the proposed biosensor to the same samples. The correlation analysis showed that the slope and r were 0.963 and 0.988, respectively, demonstrating the accuracy of cortisol quantification with our device.

Table 1. Performance Comparison of Cortisol Detection in a Spiked Artificial Sweat Sample Based on the Proposed Biosensor and ELISA Kit

spiked concentration (ng/mL)	found cortisol by the biosensor (ng/mL)	recovery of the biosensor	found cortisol by ELISA (ng/mL)	recovery of ELISA
50	54.9 ± 6.3%	109.8	53.7 ± 6.5%	107.4
100	108.6 ± 5.4%	108.6	113.7 ± 4.3%	113.7
250	267.7 ± 5.8%	107.1	242.4 ± 5.4%	97.0
500	499.3 ± 4.5%	99.9	477.6 ± 4.1%	95.5
750	768.2 ± 2.2%	102.4	746.9 ± 1.4%	99.6
1000	1019.9 ± 2.6%	102.0	976.8 ± 2.2%	97.7

Selectivity and On-Body Measurements. Negative control experiments were conducted to check the selectivity of the proposed cortisol biosensor against other chemicals present in sweat (glucose, uric acid, lactic acid, ascorbic acid, Na^+, K^+, and corticosterone). As shown in Figure 5e, cortisol generated a significant variation in fluorescence, while all the other chemicals produced little responses, even at a higher concentration. The results exhibited excellent selectivity for cortisol and indicated that the coexistence of main chemicals and related nonspecific steroids in sweat did not interfere with the detection. More substances present in sweat can be tested in future work to further investigate the selectivity.

In addition, an on-body human test was carried out by attaching our biosensor on the surface of the body via Kinesio Taping, which is easy to wear and remove. The tests were approved by the Ethical Committee of UESTC, and all the subjects have signed the consent form for the data acquisition. A ready-to-use 3D origami microfluidic chip was attached on the volunteer's wrist or neck to collect sweat at moderate exercise intensity (Figure 5f). The collected sweat samples were tested on the proposed portable biosensor and validated with ELISA. The variation range of cortisol in volunteers' sweat was 20.4−109.3 ng/mL with a relative standard deviation between 4.52 and 6.18%, and high correlation with the results of ELISA was obtained (Figure 5g).

CONCLUSIONS

In this study, we proposed a portable, inexpensive, and convenient biosensor for cortisol detection in human sweat based on the combination of fluorescently labeled aptamers and two-dimensional nanomaterials. The determination of cortisol was achieved on a 3D origami microfluidic chip via the fluorescence analysis by a smartphone mounted in the custom-made optical device. This portable device allowed the FRET analysis in the detection of the cortisol level in human sweat with a significantly reduced sample volume (20 μL), making it suitable for use in a variety of settings outside the laboratory. All experimental results showed that such a portable biosensor possessed good sensitivity, specificity, and accuracy in sweat solution with an LOD of 6.76 ng/mL (artificial sweat), demonstrating the great potential for point-of-care applications in clinical diagnostics of psychological stress and health management. Future efforts are being focused on extending the dynamic concentration range, detection sensitivity, and extensive validation against currently available protocols to meet the specific requirements of point-of-care clinical settings.

AUTHOR INFORMATION

Corresponding Author

Hai Jiang − *School of Mechanical and Electrical Engineering, University of Electronic Science and Technology of China, Chengdu, Sichuan 611731, China; Institute of Electronic and Information Engineering of UESTC in Guangdong, Dongguan, Guangdong 523808, China;* orcid.org/0000-0003-3265-5397; Email: haijiang@uestc.edu.cn

Authors

Xuan Weng − *School of Mechanical and Electrical Engineering, University of Electronic Science and Technology of China, Chengdu, Sichuan 611731, China; Institute of Electronic and Information Engineering of UESTC in Guangdong, Dongguan, Guangdong 523808, China;* orcid.org/0000-0002-3135-6099

Zhuoyi Fu − *School of Mechanical and Electrical Engineering, University of Electronic Science and Technology of China, Chengdu, Sichuan 611731, China*

Cheng Zhang − *School of Mechanical and Electrical Engineering, University of Electronic Science and Technology of China, Chengdu, Sichuan 611731, China*

Wen Jiang − *School of Mechanical and Electrical Engineering, University of Electronic Science and Technology of China, Chengdu, Sichuan 611731, China*

Complete contact information is available at:

https://doi.org/10.1021/acs.analchem.1c04508
Anal. Chem. 2022, 94, 3526−3534

https://pubs.acs.org/10.1021/acs.analchem.1c04508

Notes

The authors declare no competing financial interest.

■ ACKNOWLEDGMENTS

This work was supported by National Natural Science Foundation of China (no. 31771078), International Science, Technology and Innovation Cooperation Foundation of Sichuan Province (nos. 2020YFH0032 and 2021YFH0067), Guangdong Basic and Applied Basic Research Foundation (nos. 2021A1515010681 and 2021A1515010910), and Fundamental Research Funds for the Central Universities (nos. ZYGX2019J036 and ZYGX2020J008).

■ REFERENCES

(1) Kim, Y. M.; Cho, S. I. *Am. J. Ind. Med.* **2020**, *63*, 703−712.
(2) Reschke-Hernández, A. E.; Okerstrom, K. L.; Bowles Edwards, A.; Tranel, D. *J. Neurosci. Res.* **2017**, *95*, 106−114.
(3) Christensen, D. S.; Dich, N.; Flensborg-Madsen, T.; Garde, E.; Hansen, Å. M.; Mortensen, E. L. *Brain Behav.* **2019**, *9*, No. e01386.
(4) Nath, R. K.; Thapliyal, H.; Caban-Holt, A. *J. Signal Process Sys.* **2021**, 1−13.
(5) Kaushik, A.; Vasudev, A.; Arya, S. K.; Pasha, S. K.; Bhansali, S. *Biosens. Bioelectron.* **2014**, *53*, 499−512.
(6) Sherman, G. D.; Mehta, P. H. *Curr. Opin. Microbiol.* **2020**, *33*, 227−232.
(7) Dhull, N.; Kaur, G.; Gupta, V.; Tomar, M. *Sens. Actuators, B* **2019**, *293*, 281−288.
(8) Cesta, C. E.; Johansson, A. L. V.; Hreinsson, J.; Rodriguez-Wallberg, K. A.; Olofsson, J. I.; Holte, J.; Wramsby, H.; Wramsby, M.; Cnattingius, S.; Skalkidou, A.; Nyman Iliadou, A. *Acta Obstet. Gynecol. Scand.* **2018**, *97*, 258−268.
(9) Sekar, M.; Sriramprabha, R.; Sekhar, P. K.; Bhansali, S.; Ponpandian, N.; Pandiaraj, M.; Viswanathan, C. *J. Electrochem. Soc.* **2020**, *167*, No. 067508.
(10) Luceri, F.; Fattori, S.; Luceri, C.; Zorn, M.; Mannaioni, P.; Messeri, G. *Clin. Chem. Lab. Med.* **2001**, *39*, 1234−1239.
(11) Tang, W.; Yin, L.; Sempionatto, J. R.; Moon, J. M.; Teymourian, H.; Wang, J. *Adv. Mater.* **2021**, *33*, 2008465.
(12) Yamaguchi, M.; Matsuda, Y.; Sasaki, S.; Sasaki, M.; Kadoma, Y.; Imai, Y.; Niwa, D.; Shetty, V. *Biosens. Bioelectron.* **2013**, *41*, 186−191.
(13) Jiang, H.; Sun, Z.; Guo, Q.; Weng, X. *Biosensors and Bioelectronics* **2021**, *182*, 113191.
(14) Jiang, H.; Sun, Z.; Zhang, C.; Weng, X. *Sensors and Actuators B: Chemical* **2022**, *354*, 131232.
(15) Russell, E.; Koren, G.; Rieder, M.; Van Uum, S. H. *Ther. Drug Monit.* **2014**, *36*, 30−34.
(16) Xing, S.; Jiang, J.; Pan, T. *Lab Chip* **2013**, *13*, 1937−1947.
(17) Cheng, C.; Li, X.; Xu, G.; Lu, Y.; Low, S. S.; Liu, G.; Zhu, L.; Li, C.; Liu, Q. *Biosens. Bioelectron.* **2021**, *172*, 112782.
(18) Madhu, S.; Anthuuvan, A. J.; Ramasamy, S.; Manickam, P.; Bhansali, S.; Nagamony, P.; Chinnuswamy, V. *ACS Appl. Electron. Mater.* **2020**, *2*, 499−509.
(19) Sun, B.; Gou, Y.; Ma, Y.; Zheng, X.; Bai, R.; Abdelmoaty, A. A. A.; Hu, F. *Biosens. Bioelectron.* **2017**, *88*, 55−62.
(20) Khan, M. S.; Misra, S. K.; Wang, Z.; Daza, E.; Schwartz-Duval, A. S.; Kus, J. M.; Pan, D.; Pan, D. *Anal. Chem.* **2017**, *89*, 2107−2115.
(21) Apilux, A.; Rengpipat, S.; Suwanjang, W.; Chailapakul, O. *J. Pharm. Biomed. Anal.* **2020**, *178*, 112925.
(22) Dalirirad, S.; Steckl, A. J. *Sens. Actuators, B* **2019**, *283*, 79−86.
(23) Pinto, V.; Sousa, P.; Catarino, S. O.; Correia-Neves, M.; Minas, G. *Biosens. Bioelectron.* **2017**, *90*, 308−313.
(24) Vinitha, T. U.; Ghosh, S.; Milleman, A.; Nguyen, T.; Ahn, C. H. *Lab Chip* **2020**, *20*, 1961−1974.
(25) Jo, S.; Lee, W.; Park, J.; Kim, W.; Kim, W.; Lee, G.; Lee, H.; Hong, J.; Park, J. *Sens. Actuators, B* **2020**, *304*, 127424.
(26) Choi, J.; Bandodkar, A. J.; Reeder, J. T.; Ray, T. R.; Turnquist, A.; Kim, S. B.; Nyberg, N.; Hourlier-Fargette, A.; Model, J. B.; Aranyosi, A. J.; Xu, S.; Ghaffari, R.; Rogers, J. A. *ACS Sens.* **2019**, *4*, 379−388.
(27) Kinnamon, D.; Ghanta, R.; Lin, K. C.; Muthukumar, S.; Prasad, S. *Sci. Rep.* **2017**, *7*, 1−13.
(28) Martin, J. A.; Smith, J. E.; Warren, M.; Chávez, J. L.; Hagen, J. A.; Kelley-Loughnane, N. *J. Visualized Exp.* **2015**, *96*, E52545.
(29) Ma, H.; Shen, Z.; Ben, S. *J. Colloid Interface Sci.* **2018**, *517*, 204−212.
(30) Zhu, C.; Zeng, Z.; Li, H.; Li, F.; Fan, C.; Zhang, H. *J. Am. Chem. Soc.* **2013**, *135*, 5998−6001.
(31) Lu, Z.; Chen, X.; Hu, W. *Sens. Actuators, B* **2017**, *246*, 61−67.
(32) Wang, Y.; Ma, T.; Ma, S.; Liu, Y.; Tian, Y.; Wang, R.; Jiang, Y.; Hou, D.; Wang, J. *Microchim. Acta* **2017**, *184*, 203−210.
(33) Barua, S.; Dutta, H. S.; Gogoi, S.; Devi, R.; Khan, R. *ACS Appl. Nano Mater.* **2017**, *1*, 2−25.
(34) VanVunakis, H.; Levine, L. Use of the Double Antibody and Nitrocellulose Membrane Filtration Techniques to Separate Free Antigen from Antibody Bound Antigen in Radioimmunoassays. In *Immunoassays for Drugs Subject to Abuse*; Chapman and Hall/CRC, 2019, pp. 23−35.
(35) Cao, Q.; Liang, B.; Tu, T.; Wei, J.; Fang, L.; Ye, X. *RSC Adv.* **2019**, *9*, 5674−5681.
(36) Li, H.; Steckl, A. J. *Anal. Chem.* **2018**, *91*, 352−371.
(37) Hogenelst, K.; Soeter, M.; Kallen, V. *Sensing and Bio-Sensing Research* **2019**, *22*, 100249.